

## Propulsive performance of a finite-temperature plasma flow in a magnetic nozzle with applied azimuthal current

Lorenzo Ferrario, Justin M. Little, and Edgar Y. Choueiri

Citation: *Physics of Plasmas* **21**, 113507 (2014); doi: 10.1063/1.4901587

View online: <http://dx.doi.org/10.1063/1.4901587>

View Table of Contents: <http://scitation.aip.org/content/aip/journal/pop/21/11?ver=pdfcov>

Published by the *AIP Publishing*

---

### Articles you may be interested in

[Helicon thruster plasma modeling: Two-dimensional fluid-dynamics and propulsive performances](#)

*Phys. Plasmas* **20**, 043512 (2013); 10.1063/1.4798409

[Increased atomic hydrogen flux from a cascaded arc plasma source by changing the nozzle geometry](#)

*Appl. Phys. Lett.* **86**, 101501 (2005); 10.1063/1.1879112

[Multi-Megawatt MPD Plasma Source Operation and Modeling for Fusion Propulsion Simulations](#)

*AIP Conf. Proc.* **699**, 336 (2004); 10.1063/1.1649591

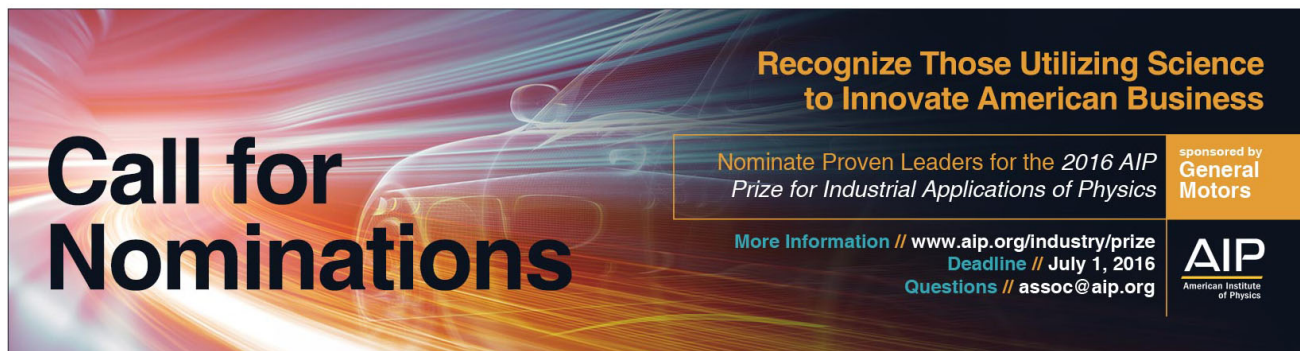
[Low Reynolds Number Performance Comparison of an Underexpanded Orifice and a DeLaval Nozzle](#)

*AIP Conf. Proc.* **663**, 557 (2003); 10.1063/1.1581594

[Numerical simulation of magnetically-guided plasma flows for the design of a fusion propulsion system](#)

*AIP Conf. Proc.* **552**, 900 (2001); 10.1063/1.1358026

---



**Call for Nominations**

**Recognize Those Utilizing Science to Innovate American Business**

Nominate Proven Leaders for the 2016 AIP Prize for Industrial Applications of Physics

More Information // [www.aip.org/industry/prize](http://www.aip.org/industry/prize)  
Deadline // July 1, 2016  
Questions // [assoc@aip.org](mailto:assoc@aip.org)

sponsored by General Motors

**AIP**  
American Institute of Physics

# Propulsive performance of a finite-temperature plasma flow in a magnetic nozzle with applied azimuthal current

Lorenzo Ferrario,<sup>1,a)</sup> Justin M. Little,<sup>2,b)</sup> and Edgar Y. Choueiri<sup>2,c)</sup>

<sup>1</sup>Politecnico di Milano, Milan 20133, Italy

<sup>2</sup>Electric Propulsion and Plasma Dynamics Laboratory, Princeton University, Princeton, New Jersey 08540, USA

(Received 12 June 2014; accepted 1 November 2014; published online 17 November 2014)

The plasma flow in a finite-electron-temperature magnetic nozzle, under the influence of an applied azimuthal current at the throat, is modeled analytically to assess its propulsive performance. A correction to the nozzle throat boundary conditions is derived by modifying the radial equilibrium of a magnetized infinite two-population cylindrical plasma column with the insertion of an external azimuthal body force for the electrons. Inclusion of finite-temperature effects, which leads to a modification of the radial density profile, is necessary for calculating the propulsive performance, which is represented by nozzle divergence efficiency and thrust coefficient. The solutions show that the application of the azimuthal current enhances all the calculated performance parameters through the narrowing of the radial density profile at the throat, and that investing power in this beam focusing effect is more effective than using the same power to pre-heat the electrons. The results open the possibility for the design of a focusing stage between the plasma source and the nozzle that can significantly enhance the propulsive performance of electron-driven magnetic nozzles. © 2014 AIP Publishing LLC. [<http://dx.doi.org/10.1063/1.4901587>]

## I. INTRODUCTION

A Magnetic Nozzle (MN) is a propulsive device that converts part of the thermal energy of a plasma into direct kinetic energy. Application of such nozzles can be found in fundamental plasma physics experiments,<sup>1</sup> plasma processes,<sup>2–4</sup> and plasma propulsion for spacecraft.<sup>5–12</sup>

The underlying mechanism in such devices relies on high plasma conductivity.<sup>13</sup> This so called frozen-in condition forces the plasma to follow the magnetic stream surfaces as they expand through the nozzle. This property allows the magnetic nozzle to guide the plume much like the gasdynamic expansion in conventional rocket nozzles. The momentum is then transferred back to the thruster by the mutual interaction of induced diamagnetic currents in the plume and the applied magnetic field.<sup>8</sup>

The flexibility of MNs allowed a number of proposed concepts in plasma propulsion, such as helicon thrusters,<sup>14</sup> permanent magnet micropropulsion systems for cubesat,<sup>15</sup> VASIMR architecture,<sup>5</sup> and proposed fusion rockets.<sup>16,17</sup>

The absence of electrodes, often identified as the life-limiting components of other electric propulsion systems,<sup>18</sup> and the ability to scale to high power<sup>5</sup> make the MN a desirable option for the acceleration stage for pre-ionized gaseous propellants.

When the thermal energy is stored mainly in the electrons ( $T_e \gg T_i$ ), the functioning mechanism can be described as *thermal* for the electrons fluid and *electrostatic* for the ions. We refer to such devices as Electron-Driven Magnetic Nozzles (EDMN).<sup>12</sup> In this class of magnetic nozzles, the thermal energy stored in the electrons drives them in a

thermal expansion in the divergent field. The ions, on the contrary, are much cooler and tend not to undergo the same thermal acceleration. Therefore, an ambipolar electric field arises to conserve local quasi-neutrality<sup>19</sup> and electrostatically accelerates ions, thus producing thrust.

## A. Open problems in magnetic nozzle theory

While MNs have been already implemented in various thruster prototype architectures,<sup>5,14–17</sup> their governing physics have yet to be fully understood and the plasma dynamics in MNs are still an active field of research.

Among other problems, plasma detachment is a central issue affecting thrust production in MN and has been investigated through a number of simulations<sup>10,11,20</sup> and analytical models.<sup>6,7,21</sup> Recently, Deline *et al.*<sup>22</sup> provided the first experimental evidence of plasma detachment in such MNs flows. However, the divergence in plasma flow in MNs has an obvious adverse effect in thrust production and nozzle efficiency.

How and where this detachment occurs is still under a vivid scientific debate. Previously accepted theories of resistive<sup>7</sup> and electron inertia<sup>6</sup> detachment mechanism have recently been questioned,<sup>10,11</sup> while experimental measurements<sup>5</sup> did not verify the stretching to the infinite of the magnetic field lines as foreseen by Arefiev and Breizman.<sup>21</sup>

Other problems affecting MNs-based thrusters are poor thermal-kinetic power conversion efficiency<sup>23</sup> at low power and magnetic field and poor ionization.

## B. Motivation and scope

In their paper,<sup>9</sup> Schmit and Fisch expanded Hooper's<sup>6</sup> nozzle model, introducing an azimuthal current that couples

<sup>a)</sup>lorenzo.ferrario@polimi.it

<sup>b)</sup>jml@princeton.edu. URL: <http://alfven.princeton.edu>

<sup>c)</sup>choueiri@princeton.edu

with the axial magnetic field to produce a significant decrease in the plume divergence.

However, through numerical solution of a finite-temperature plasma flow model, Ahedo and Merino<sup>10</sup> showed that the hypotheses of negligible pressure effect and absent ambipolar current used by Hooper's model do not allow an understanding of the thermal-electrostatic nature of the plasma expansion in magnetic nozzles. Moreover, as a consequence of this analysis, it became clear that to assess the effect of an applied azimuthal current, a finite-temperature model of the plasma flow must be used. Thus, in this paper, we wish to extend Schmit and Fisch's idea to Ahedo and Merino's model in order to have a more complete description of the interaction between the azimuthal current and the plasma flow.

Schmit and Fisch showed that a decrease in the plume divergence is observed when introducing the azimuthal current and they suggest this divergence reduction leads to an increase in the nozzle efficiency. Therefore, we wish also to verify their suggestion by assessing the effects of the azimuthal current on the propulsive performance of the nozzle.

Finally, the introduction of an azimuthal current is an active process and, as such, requires some additional power to be provided to the plume. Thus, it is natural to ask if the introduction of this azimuthal current is an efficient way of recovering direct kinetic power, or, in other terms, how the direct kinetic power recovery relates to the applied power.

### C. Approach

When an azimuthal current is applied at the nozzle throat, an interaction between the resulting Lorentz force and the radial pressure expansion term arises, changing the equilibrium state of the plasma. Therefore, if we want to apply an externally-induced swirl motion to a finite-temperature model, we need also to modify the nozzle throat conditions consistently with the new equilibrium.

We start by solving the equations of an infinite plasma column in steady equilibrium, confined by an axial external magnetic field, with an applied body force in the azimuthal equation. Mathematically speaking, we are adding a variable that would eventually be defined with an additional equation. Once the new throat boundary conditions are defined, we solve the two-dimensional axisymmetric flow in the nozzle and we evaluate the effects on the nozzle performance.

By imposing the sum of the radial components of the Lorentz and the centrifugal forces to be negative

$$F_{ar}^{\theta} = q_a B_z u_{\theta a} + m_a \frac{u_{\theta a}^2}{r} < 0, \quad (1)$$

where  $q_a$  and  $m_a$  are the charge and the mass of the  $a$ -th population,  $B_z$  is the axial magnetic field, and  $u_{\theta a}$  is the azimuthal velocity; we can find a condition on the angular velocity at the nozzle throat ( $\omega_a^t = u_{\theta a}^t / R^t$ , where  $R^t$  is the radial position of the streamline at the throat) of each species streamline by which such radial force has a net collimating effect. Using the superscript  $t$  to indicate the quantities at the throat, we get

$$-\Omega_z \frac{r^2}{R_a^2} - 2 \frac{q_a}{m_a R_a^2} (\psi^t - \psi) < \omega_a^t < 0, \quad (2)$$

where  $\Omega_z$  is the local cyclotron frequency magnitude of the  $a$ -th species, computed with the axial magnetic field  $B_z$ , and  $\psi$  is the magnetic streamfunction, defined according to

$$\mathbf{B} = \frac{1}{r} (\hat{\vartheta} \times \nabla \psi). \quad (3)$$

We can specialize the equations for two species (electrons and ions) plasma. In this situation, we know that  $\psi^0 - \psi \geq 0$  for the ions, due to their inward separation from the magnetic streamlines,<sup>10</sup> and  $\psi^0 - \psi \approx 0$  for the electrons,<sup>11</sup> due to their high magnetization, typical of most of the practical applications of EDMNs.<sup>1,5</sup> Therefore, since  $r \geq R^0$  along all the divergent streamline, the strictest condition is found at the nozzle throat and reads

$$\begin{cases} -\Omega_i^0 < \omega_i^0 < 0 \\ 0 < \omega_e^0 < \Omega_e^0. \end{cases} \quad (4)$$

If these inequalities are met, the radial component of the Lorentz force dominates over the centrifugal force, leading to a net collimating effect along all the streamline.

From condition (4), we see that electrons have a range of admissible angular velocities that is much wider than that of the ions. Thus, differently from Schmit and Fisch,<sup>9</sup> we will focus our attention on the electron fluid only, also because is easier for the electrons to carry the current.<sup>24-26</sup>

### D. Paper outline

This paper is organized as follows: first, the radial equilibrium in an infinite magnetized plasma column with the presence of an electron azimuthal body force is modeled analytically. Then, the solution is used as boundary condition at the throat of a magnetic nozzle, and the flow in the divergent section is computed using an analytical approximation. In the Sec. IV, the effects of the introduced electron body force on the nozzle propulsive performances are presented and discussed.

## II. NOZZLE THROAT BOUNDARY CONDITIONS IN SWIRLING REGIME

### A. Equilibrium equations for an infinite column of magnetized plasma

We consider an infinite cylindrical plasma column with an externally-applied axial magnetic field. In this section, we modify the equilibrium equations of Ahedo<sup>27</sup> to include the effect of an externally-applied azimuthal body force  $F$ .

The plasma in our model consists of electrons and singly-charged ions. We assume the sheath length scale to be much smaller than the radius of the plasma column, thus the plasma remains quasi-neutral  $n_e = n_i = n$  within the domain of our model. We consider the limit  $\beta \ll 1$ , where  $\beta$  is the ratio of the plasma thermal energy density to the magnetic field energy density. This limit allows us to neglect the magnetic field induced by the diamagnetic plasma currents.<sup>28</sup>

Following Ahedo,<sup>27</sup> we assume equal radial velocities of electrons and ions  $u_{ri} = u_{re} = u_r$ . This is generally true in the plasma central region, where the charge-separating electric field of the sheath is not yet significant. Our attention is mainly focused here because the propulsive performance of the nozzle is mostly influenced by this region.<sup>10</sup> With this in mind, the plasma behavior in the sheath will not be investigated in this study.

The modified momentum equation in cylindrical coordinates  $(r, \theta, z)$ , assuming axisymmetry  $(\partial/\partial\theta = 0)$  and dropping the axial derivatives  $(\partial/\partial z = 0)$  in the azimuthal direction for the electrons is<sup>27</sup>

$$m_e u_r \frac{du_{\theta e}}{dr} + m_e \frac{u_{\theta e} u_r}{r} = e B u_r - m_e (\nu_{en} + \nu_w) u_{\theta e} - m_e \nu_{ei} (u_{\theta e} - u_{\theta i}) + F, \quad (5)$$

where  $\nu_{en}$ ,  $\nu_{ei}$  are the electron-neutral and electron-ion collision frequencies, respectively, and  $\nu_w$  is the ion production frequency, due to axial diffusion and ionization of neutrals. We introduce  $F$  in Eq. (5) as a generalized body force acting on electrons only which induces the differential motion in the two species required to create a net azimuthal current. The other three momentum equations and the continuity equation are left unchanged:

$$m_e u_r \frac{du_r}{dr} - m_e \frac{u_{\theta e}^2}{r} = -\frac{1}{n} \frac{d}{dr} (T_e n) + e \frac{d\phi}{dr} - e B u_{\theta e} - m_e (\nu_{en} + \nu_w) u_r, \quad (6)$$

$$m_i u_r \frac{du_r}{dr} - m_i \frac{u_{\theta i}^2}{r} = -\frac{1}{n} \frac{d}{dr} (T_i n) + e \frac{d\phi}{dr} + e B u_{\theta i} - m_i (\nu_{in} + \nu_w) u_r, \quad (7)$$

$$m_i u_r \frac{du_{\theta i}}{dr} + m_i \frac{u_{\theta i} u_r}{r} = -e B u_r - m_i (\nu_{in} + \nu_w) u_{\theta i} + m_i \nu_{ei} (u_{\theta e} - u_{\theta i}), \quad (8)$$

$$\frac{1}{r} \frac{d}{dr} (r n u_r) = n \nu_w. \quad (9)$$

In accordance with Ahedo,<sup>27</sup> we drop the electric potential gradient in the plasma bulk region  $(\nabla\phi = 0)$  and nondimensionalize the equations using the radial location of the sheath,  $R_s$ , the sonic speed  $c_s = \sqrt{T_e/m_i}$ , the density on the axis  $n_0$ , and the electron energy  $T_e$ . We further assume that  $T_e$  is constant over the plasma cross-section.

An exception to this normalization scheme is the electron azimuthal velocity, which is given the following dimensionless form:

$$\hat{u}_{\theta e} = \frac{u_{\theta e}}{c_s} \sqrt{\frac{m_e}{m_i}}. \quad (10)$$

This formalism is used to bring  $\hat{u}_{\theta e}$  to the same order as the rest of the dimensionless variables.

Manipulating Eq. (5), dropping the inertial terms, and applying the hypotheses of cold ions  $(T_i \approx 0)$ <sup>10–12,27</sup> and negligible ion azimuthal motion  $(u_{\theta i} \approx 0)$ ,<sup>27</sup> we get the modified expression for the radial velocity

$$\hat{u}_r = \frac{\hat{\nu}_e}{\hat{\omega}_{lh}} \hat{u}_{\theta e} - \frac{\hat{F}}{\hat{\omega}_{lh}}. \quad (11)$$

Here,  $\hat{\nu}_e = \hat{\nu}_{ei} + \hat{\nu}_{en} + \hat{\nu}_w$  with each frequency normalized by the quantity  $c_s/R_s$ . The normalized lower hybrid frequency is defined as

$$\hat{\omega}_{lh} \equiv \frac{eB}{\sqrt{m_i m_e}} \frac{R_s}{c_s}, \quad (12)$$

which is the main parameter that captures the influence of the applied magnetic field strength on the equilibrium plasma configuration.

We can see from Eq. (11) how the azimuthal body force,  $\hat{F}$ , couples with the magnetic field,  $\hat{\omega}_{lh}$ , to modify the radial velocity profile. It is clear from this equation that a positive force reduces the outward radial velocity. Physically, the positive force induces a diamagnetic current. This diamagnetic current couples with the axial magnetic field, enhances the natural inward Lorentz force, and improves the radial plasma confinement.

The radial electron momentum balance yields

$$\hat{\omega}_{lh} \hat{u}_{\theta e} = -\frac{d \ln \hat{n}}{d \hat{r}}. \quad (13)$$

Combining Eqs. (9)–(11) leads to the modified diffusion equation

$$\frac{d^2 \hat{n}}{d \hat{r}^2} + \left( \frac{1}{\hat{r}} + \frac{\hat{\omega}_{lh} \hat{F}}{\hat{\nu}_e} \right) \frac{d \hat{n}}{d \hat{r}} + \left( a_0^2 + \frac{\hat{\omega}_{lh} d \hat{F}}{\hat{\nu}_e d \hat{r}} + \frac{\hat{\omega}_{lh} \hat{F}}{\hat{\nu}_e \hat{r}} \right) \hat{n} = 0, \quad (14)$$

where

$$a_0 = \hat{\omega}_{lh} \sqrt{\frac{\hat{\nu}_w}{\hat{\nu}_e}}. \quad (15)$$

This equation is a second-order ODE that when combined with the proper boundary conditions yields the radial plasma density profile as a function of the collisionality of the plasma,  $\hat{\nu}_e$ , applied magnetic field strength,  $\hat{\omega}_{lh}$ , and azimuthal force,  $\hat{F}$ .

Again, we see from Eqs. (11) and (14) that the azimuthal body force  $\hat{F}$  acts with the magnetic field,  $\hat{\omega}_{lh}$ , to modify the diffusion equation and eventually the radial density profile of the plasma. From the same equation, we also see that the net effect of the body force is scaled by the ratio  $\hat{\omega}_{lh}/\hat{\nu}_e$ , which is the ratio of the non-dimensional magnetic field parameter to the electron global collisional term. In other words, the effect of the body force is proportional to the magnetization, which controls the strength of the Lorentz interaction, and is inversely proportional to the electron collisional term, which acts as a momentum sink for the electron population.

Finally, we adopt the on-axis boundary conditions of Ahedo:<sup>27</sup>  $\hat{n}(0) = 1$  and  $\hat{n}'(0) = 0$ . The Bohm sheath requirement,  $\hat{u}_r(1) = 1$ , determines the eigenvalue  $\hat{\nu}_w$ , where  $\hat{\nu}_w = \hat{\nu}_w(\hat{\omega}_{lh}, \hat{\nu}_e, \hat{F})$ .



## B. Application to a particular form of $\hat{F}$

We proceed by assuming a particular form of  $\hat{F}$  in order to solve Eq. (14). The quantitative results will depend strictly on this choice, but some consideration on the behavior of the plasma can be generalized to a broader class of body forces. We choose  $\hat{F}$  to be

$$\hat{F} = \hat{\Omega}\hat{r} - \hat{u}_{\theta e}, \quad (16)$$

which causes the azimuthal motion of the electrons to tend to a rigid body motion with angular frequency  $\hat{\Omega}$ . Clearly, this body force vanishes when the electrons are moving collectively at the desired angular frequency and changes sign for higher  $\hat{u}_{\theta e}$ .

We note that a positive  $\hat{\Omega}$  would induce a diamagnetic electron current, while a negative  $\hat{\Omega}$  would induce a paramagnetic one. This definition of  $\hat{F}$  resembles the effect of a Rotating Magnetic Field (RMF) configuration used to drive electron currents in fusion experiments.<sup>29</sup> Quantitatively, such a  $\hat{F}$  corresponds to a generalization of the force exerted by the RMF on the electrons within the approximation<sup>25</sup> of fixed ions and  $\hat{\Omega}_{ce}/\nu_{ei} \gg 1$ . These conditions are justified for MNs by the low residence time of the ions in the device.

Finally, we can substitute Eq. (16) into Eq. (11),

$$\hat{u}_r = \frac{\hat{\nu}_e + 1}{\hat{\omega}_{lh}} \hat{u}_{\theta e} - \frac{\hat{\Omega}\hat{r}}{\hat{\omega}_{lh}}, \quad (17)$$

and Eq. (14),

$$\frac{d^2\hat{n}}{d\hat{r}^2} + \left[ \frac{1}{\hat{r}} + \left( \frac{\hat{\omega}_{lh}\hat{\Omega}}{\hat{\nu}_e + 1} \right) \hat{r} \right] \frac{d\hat{n}}{d\hat{r}} + \left[ a_{\hat{\Omega}}^2 + 2 \left( \frac{\hat{\omega}_{lh}\hat{\Omega}}{\hat{\nu}_e + 1} \right) \right] \hat{n} = 0, \quad (18)$$

where

$$a_{\hat{\Omega}} = \hat{\omega}_{lh} \sqrt{\frac{\hat{\nu}_w}{\hat{\nu}_e + 1}}. \quad (19)$$

Equation (18) has a free parameter  $\hat{\Omega}$  and two imposed parameters  $(\hat{\nu}_e, \hat{\omega}_{lh})$ . The eigenvalue  $\hat{\nu}_w = \hat{\nu}_w(\hat{\omega}_{lh}, \hat{\nu}_e, \hat{\Omega})$ , whose value depends on the other three parameters, is computed by imposing the Bohm condition,  $\hat{u}_r(1) = 1$ , at the sheath.

## C. Solution for plasma bulk region

We can use the approximate diffusion equation, Eq. (18), to look at the effect of inducing azimuthal electron current, or swirl, on the equilibrium structure of the magnetized plasma column. We will first consider the case of no swirl, from which we recover the previously observed radial plasma structure. We will then look at the effect on the radial plasma structure of adding electron swirl in a diamagnetic sense.

*No Swirl:*  $\hat{\Omega} = 0$

Let us first consider the case of no induced electron current. Setting  $\hat{\Omega} = 0$  in Eq. (18), we recover the diffusion equation of Ahedo,<sup>27</sup> which has the solution

$$\hat{n}(\hat{r}) = J_0(a_{\hat{\Omega}}\hat{r}). \quad (20)$$

Here,  $a_{\hat{\Omega}}$  is approximately equal to the first zero of  $J_0$  to satisfy the boundary condition at the wall. From Eq. (20), the azimuthal and radial electron velocities may be obtained from Eqs. (13) and (17). These solutions for a given magnetization are shown in Fig. 1.

We note that the solution to the diffusion equation for  $\hat{\Omega} = 0$  was found earlier by Fruchtman *et al.*<sup>30</sup> without neglecting ion inertia and exhibits similar behavior to the solution to the approximate diffusion equation in the no swirl limit. Furthermore, they derived the  $\hat{\Omega} = 0$  form of Eq. (18), and its solution, Eq. (20), as a limiting case of their model in which inertial effects are negligible.

*Diamagnetic Swirl:*  $\hat{\Omega} > 0$

We can use our model to investigate the influence of an induced diamagnetic electron current or diamagnetic swirl, on the structure of the plasma column. We numerically solve

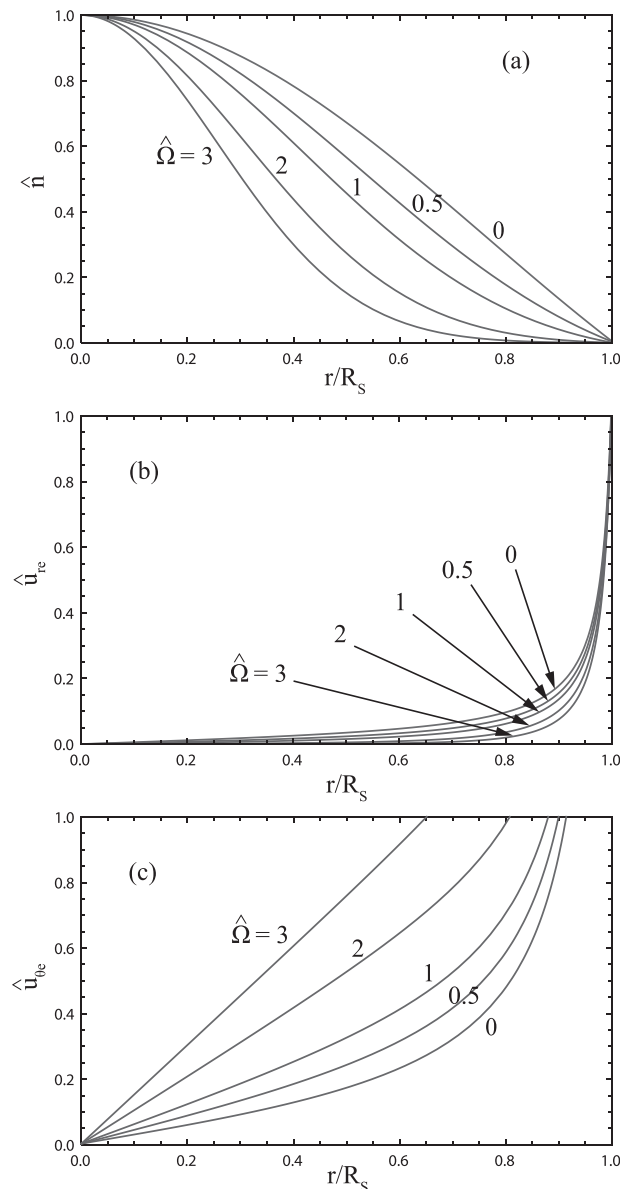


FIG. 1. Radial profile of the (a) normalized plasma density, (b) normalized radial velocity, and (c) normalized electron azimuthal velocity for different values of  $\hat{\Omega}$ . The radial coordinate is normalized by the sheath coordinate  $R_s$ . Other parameters are  $\hat{\omega}_{lh} = 10$ ;  $\hat{\nu}_e = 1$ .

Eq. (18) subject to the boundary conditions above for different values of  $\hat{\Omega}$ . The solutions are plotted in Fig. 1, where we show the radial profiles of  $\hat{n}$ ,  $\hat{u}_{\theta e}$ , and  $\hat{u}_r$  for various values of the parameter  $\hat{\Omega}$ .

It is clear from Fig. 1(a) that the radial density profile of the plasma column changes significantly even for low values of  $\hat{\Omega}$ . The resulting shape of the density distribution shows a change in the sign of the second derivative, leading to a steeper decay at greater values of  $\hat{r}$ . In other words, the bulk plasma becomes more concentrated towards the axis as the azimuthal electron current increases.

Physically, the effect of the force  $\hat{F}$  on the electrons is clear from Fig. 1(c). Here, we see that progressively higher values of  $\hat{F}$  drag the electron towards the expected rigid-body motion. As visible in Fig. 1(b), this induced azimuthal motion of the electrons counteracts the pressure push, lowering the outwardly-directed radial velocity and, eventually, resulting in a more confined radial density profile.

Now, one might correctly point out that the approximation of negligible electron inertia<sup>27</sup> is lost with higher values of  $\hat{\Omega}$ , as we can see by the expansion of the region with  $\hat{u}_{\theta e} > 1$  for increasing  $\hat{F}$ . However, we note that the plasma density in the outer region of the plasma is progressively diminished, thus lowering the effect of the plasma border on the final nozzle performance. Therefore, keeping in mind the scope of the paper, we do not expect our results to change significantly with the addition of electron inertial effects towards the plasma periphery.

### III. NOZZLE FLOW ANALYTICAL SOLUTION

With the modified solution of the magnetized plasma column, we may now compute the resulting MN flow. Specifically, we will use the radial density profile, including induced electron swirl as a boundary condition at the MN throat to solve the two-dimensional expansion of the plasma using the approximate analytical solution of Little and Choueiri<sup>12</sup> to the model of Ahedo and Merino.<sup>10</sup> The coupling of these two models is analogous to the coupling of a “focusing stage,” used to drive azimuthal electron current in the flow, and a MN “acceleration stage,” used to recover the thermal energy of the plasma for propulsion applications.

#### A. Model assumptions and governing equations

Ahedo and Merino<sup>10</sup> use a two-fluid (electrons and singly-charged ions) model for the expansion of a MN plasma. They consider MNs in which the expansion was driven mainly by the hot electrons with the ions remaining cold ( $T_i = 0$ ). By neglecting electron inertial terms they show that the electrons remain tied to the expanding magnetic field lines. Numerically solving this model for an isothermal expansion, they demonstrate that although the plasma is assumed to remain quasi-neutral everywhere, the majority of plasma ions separate inwards with respect to the expanding magnetic field.

An approximate analytical solution to the 2D model of Ahedo and Merino was recently derived by Little and Choueiri.<sup>12</sup> Motivating their solution was the observation by Ahedo and Merino that the average of the plasma potential

along the MN axis and boundary approximately follows the plasma potential predicted from quasi-1D models. Therefore, Little and Choueiri derived a solution to the 2D fluid model that consists of a quasi-1D component with a 2D, cross-field correction. In the limit of negligible ion magnetization, and by assuming the ions approximately follow the magnetic field lines, they show that this solution agrees remarkably well with the numerical results of Ahedo and Merino.

Both the model of Ahedo and Merino and the analytical approximation of Little and Choueiri use a zeroth-order Bessel function density profile [Eq. (20)] as the inlet conditions at the MN throat. As we mentioned early, this profile is the equilibrium condition for an infinite magnetized plasma in the limit, where inertial forces are negligible. For our analysis of the performance MN thrusters with applied azimuthal electron current, we will instead use the equilibrium density profile derived in Sec. II as the MN throat inlet conditions in the solution of Little and Choueiri.

The solution uses a transformation from cylindrical ( $r, z$ ) to magnetic ( $\psi, \zeta$ ) coordinates, where  $\psi$  is the magnetic stream function and  $\zeta$  is the magnetic scalar potential. The relationship between the magnetic field and these scalar quantities is given by<sup>31</sup>

$$\mathbf{B} = \frac{1}{r} (\hat{\vartheta} \times \nabla \psi) = -\nabla \zeta. \quad (21)$$

We will also adapt the magnetic field model used by Little and Choueiri, Eqs. (26) and (27) in Ref. 12, which is a good approximation for plasma expansion through a dipole magnetic field (Fig. 2).

We note that in contrast to the cylindrical plasma column model, length scales in the MN model are normalized by the radius of the magnet,  $R_m$ , as opposed to the radial location of the sheath,  $R_s$ . Although the other normalizations are kept the same, we switch to a tilde notation to avoid confusion (i.e.,  $\tilde{r} = r/R_m$ ). As a result of the coupling between the two models, the radius of the plasma entering the MN,  $\tilde{r}_p \equiv R_s/R_m$ , becomes an important quantity because it determines the divergence of the bounding magnetic flux surface,  $\tilde{\psi}_p$ .

The coordinate transformation allows Little and Choueiri to separate the solution into a  $\psi$ -averaged component, obtained from a quasi-1D model, and a  $\psi$ -dependent correction, obtained from the ion force balance along constant  $\zeta$ . The latter equation takes the form

$$\frac{\partial \tilde{\phi}}{\partial \tilde{\psi}} = -\frac{\tilde{M}_i^2}{\tilde{r} \tilde{B} \tilde{R}_c} + \frac{1}{\tilde{\rho}_{L,i}} \frac{\tilde{u}_{\theta i}}{\tilde{r}}. \quad (22)$$

Here,  $\tilde{R}_c$  is the local curvature radius of the magnetic field,  $\tilde{\rho}_{L,i} \equiv m_i c_s / (e B_0)$  is the modified ion Larmor radius, and  $\tilde{M}_i \equiv \tilde{\mathbf{u}}_i \cdot \tilde{\mathbf{b}}$  is the ion Mach number projected on magnetic field unit vector,  $\tilde{\mathbf{b}}$ . Equation (22) states that equilibrium requires the force due to the ambipolar electric field (left-hand side) balances the ion dynamic pressure force (first term on right-hand side) and ion Lorentz force (second term on right-hand side).

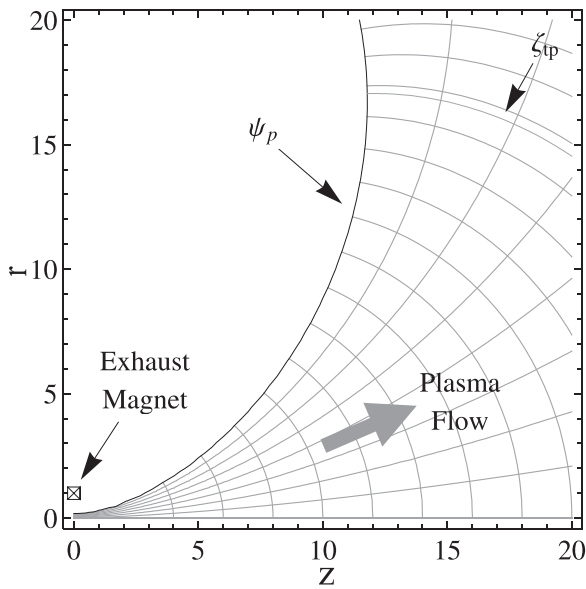


FIG. 2. Magnetic nozzle field topology. The grid shows the transformation from geometric  $(r, z)$  to magnetic  $(\psi, \zeta)$  coordinates. The plasma-vacuum interface is marked by the stream coordinate  $\psi_p$ , which is shown here for  $\tilde{r}_p = 0.185$ . The plasma-vacuum magnetic surface turning point has the coordinate  $\zeta_{tp}$ . Reprinted with permission from J. M. Little and E. Y. Choueiri, “Thrust and efficiency model for electron-driven magnetic nozzles”, *Phys. Plasmas* **20**, 103501 (2013). Copyright 2013, American Institute of Physics.<sup>12</sup>

Similar to Little and Choueiri, we consider the limit of  $\tilde{\rho}_{L,i} \gg 1$ , which allows us to neglect the influence of the ion Lorentz force. We retain this term for a moment, however, to obtain a qualitative understanding of the effect of electron and ion rotation on the MN exhaust plume. Combining Eq. (22) with the electron cross-field force balance yields

$$\frac{1}{\tilde{n}} \frac{\partial \tilde{n}}{\partial \tilde{\psi}} = -\frac{\tilde{M}_i^2}{\tilde{r} \tilde{B} \tilde{R}_c} + \frac{1}{\tilde{r}} \left( \frac{\tilde{u}_{\theta i}}{\tilde{\rho}_{L,i}} - \frac{\tilde{u}_{\theta e}}{\tilde{\rho}_{L,e}} \right), \quad (23)$$

where  $\tilde{\rho}_{L,e}$  is the normalized electron Larmor radius. The term on the right hand side represents the gradient of the density profile along constant  $\zeta$ , and becomes more negative as the plasma is focused towards MN axis. It is clear that the ion dynamic pressure increases the relative focusing of the plume. This effect is more pronounced for magnetic fields that rapidly diverge (large  $\tilde{R}_c$ ) or large ion kinetic energies (large  $\tilde{M}_i$ ). The ion Lorentz force tends to de-focus the exhaust plume because it counteracts ion motion across the magnetic fields.

The effect of the focusing stage is to increase  $\tilde{u}_{\theta e}$  above its natural value, as demonstrated in Fig. 1(c). Ahedo and Merino<sup>11</sup> showed that for an equilibrium plasma profile given along a cross-sectional flow plane,  $\tilde{u}_{\theta e}$  is uniquely determined everywhere by only the magnetic topology. This results from the fact that the quantity  $\tilde{u}_{\theta e}/\tilde{r}$  is conserved along  $\tilde{\psi}$ . As a consequence, the Lorentz force term in Eq. (23) is also conserved along the magnetic flux surface. This implies that the main effect of the focusing stage is to alter the equilibrium plasma profile entering the MN—an effect that is then propagated downstream. The increased electron azimuthal velocity does not, however, continue to collimate

the expanding plasma beyond the focusing stage. This would also imply that the power spent on swirling the electrons is not recovered in the nozzle. We will examine the tradeoff between the power used in the focusing stage and the increased efficiency of the nozzle in Sec. IV.

In summary, we conclude that the presence of an azimuthal current influences the two-dimensional density distribution inside the magnetic nozzle in two ways: the ion azimuthal current and kinetic energy recovery induce a change in the potential profile across the magnetic streamlines, while the electron current changes the boundary conditions at the nozzle throat. This represents a marked difference with what was previously observed by Schmit and Fisch.<sup>9</sup> According to our theory, the effect of introducing an electron swirling motion is manifested at the location where the external force occurs. The modified equilibrium state is then propagated throughout the plume in the divergent part of the nozzle due to the hyperbolic nature of the supersonic fluid equations. Thus, the modified radial density distribution propagates along the nozzle, even outside the region of influence of  $F$ . This makes it clear that the actual effect of an azimuthal current cannot be correctly modeled by using a zero-temperature model. Indeed, in such a case, the radial Lorentz force induced by the swirling would not be balanced a pressure force, leading to a non-equilibrium situation.

## B. Density profile scaling

We use the radial density profile obtained from the focusing stage model as the entrance condition for the MN model to analyze the effect of induced azimuthal electron currents on the divergence of the exhaust plume. To allow a direct comparison, we scale the density profile such that the mass flow rate into the MN is constant with varying  $\hat{\Omega}$ . Denoting the density profile at the MN throat as  $\tilde{n}_t(\tilde{r}, \hat{\Omega})$ , this may be written symbolically as

$$\tilde{n}_t(\tilde{r}, \hat{\Omega}) = \rho(\hat{\Omega}) \tilde{n}_t(\tilde{r}, 0), \quad (24)$$

where the scaling factor can be found from

$$\rho(\hat{\Omega}) = \int_0^1 \hat{r} \hat{n}_t(\hat{r}, 0) d\hat{r} / \int_0^1 \hat{r} \hat{n}_t(\hat{r}, \hat{\Omega}) d\hat{r}. \quad (25)$$

In Fig. 3, we show two effects of the application of  $F$ : a compression of the plasma bulk region and, for mass flux conservation, the increase in the density peak value in the throat center.

## C. Magnetic nozzle flow in electron swirling regime

Having modified the MN entrance condition in accordance with the focusing stage model, we can compare the new results with the baseline, no-swirling solution of Little and Choueiri.<sup>12</sup> This comparison is shown in Fig. 4 using contour plots of the density for (a)  $\hat{\Omega} = 0$  and (b)  $\hat{\Omega} = 5$ . We observe that with the addition of swirling electrons, the flow has more elongated density lobes. Furthermore, the density decays faster near the boundary because the cross-field derivative is higher in magnitude. Therefore, the power used

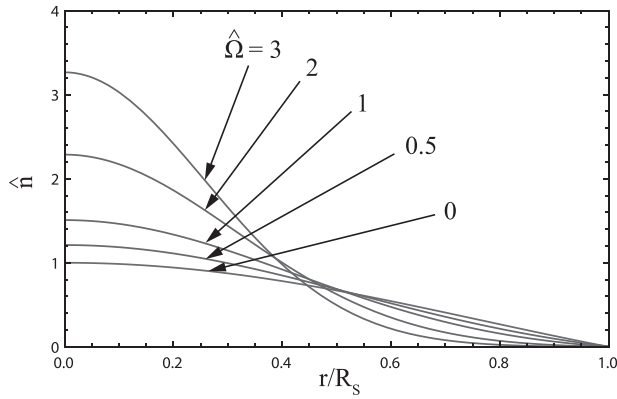


FIG. 3. Change in the non-dimensional plasma radial density profile at the throat with  $\hat{\Omega}$ , when the flux-conserving scaling is applied. The baseline is for  $\hat{\Omega} = 0$ . Magnetization parameter  $\hat{\omega}_{lh} = 10$ .

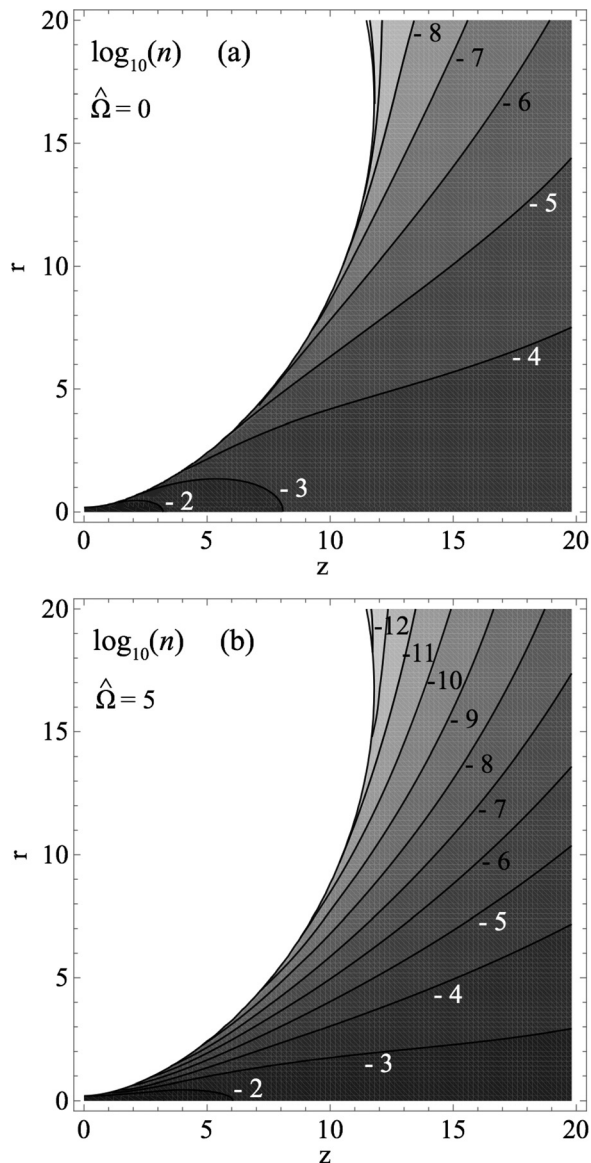


FIG. 4. Maps of plasma density for (a)  $\hat{\Omega} = 0$  and (b)  $\hat{\Omega} = 5$ . Here,  $\tilde{r}_p = 0.185$ ,  $\hat{\omega}_{lh} = 10$ , and  $\tilde{\nu}_e = 1$ .

to drive the azimuthal electron current produces a more collimated exhaust plume.

#### IV. PROPULSIVE PERFORMANCE ASSESSMENT

In this last section, we use the modified nozzle flow solution to assess the effects of the swirling on the propulsive performances of the magnetic nozzle. Furthermore, we address the questions: *does the decreased plume divergence offset the power required to drive the azimuthal current?*, and, *would that power be better spent simply heating the electrons?*

##### A. Performance metrics

The divergence efficiency of a MN,  $\eta_{div}$ , is defined as the ratio of the axial kinetic power,  $P_b^*$ , to the total kinetic power,  $P_b$ , in the exhaust. After Little and Choueiri,<sup>12</sup> we calculate this value at the plane that corresponds to the turning point of the magnetic field defined by  $\zeta_{tp} = \tilde{\zeta}_{tp}$  (see Fig. 2). Within the framework of the MN model, the divergence efficiency may be written symbolically as

$$\eta_{div} \equiv \frac{P_b^*}{P_b} = \frac{\int_{\zeta_{tp}} \tilde{n} \tilde{M}_i^3 \frac{\tilde{B}_z^2}{\tilde{B}^2} d\tilde{A}}{\int_{\zeta_{tp}} \tilde{n} \tilde{M}_i^3 d\tilde{A}}, \quad (26)$$

where the  $\tilde{B}_z/\tilde{B}$  ratio comes from the approximation  $\tilde{M}_{i,z} \approx \tilde{M}_i(\tilde{B}_z/\tilde{B})$ .

This divergence efficiency is related to the overall thrust efficiency,  $\eta_t$ , through the relation  $\eta_t = \eta_i \eta_{div}$ , where  $\eta_i$  takes into account all other loss mechanisms. It is clear that plume focusing affects mainly  $\eta_{div}$ , however,  $\eta_i$  might also benefit. In the case of helicon plasma sources, the focusing stage could improve the antenna-plasma coupling<sup>32,33</sup> and reduce wall losses.<sup>34</sup>

The MN thrust coefficient,  $C_T$ , is defined as the ratio of the thrust to the pressure force at the MN throat. This can be written as

$$C_T = \frac{1}{\langle \tilde{n}_t \rangle \tilde{A}_t} \int_{\zeta_{tp}} \tilde{n} (\tilde{M}^2 + 1) \frac{\tilde{B}_z}{\tilde{B}} d\tilde{A}, \quad (27)$$

where  $\langle \tilde{n}_t \rangle = \int \tilde{n}_t d\tilde{A} / \tilde{A}_t$  is the mean density at the throat plane. A normalized specific impulse may be defined such that  $\hat{I}_{sp} \equiv g_0 I_{sp} / c_s = \eta_m C_T$ , where  $\eta_m$  is the mass utilization efficiency of the thruster defined as the ratio of the ion mass flow rate leaving the MN,  $\dot{m}_i$ , to the total mass flow rate,  $\dot{m}$ . Therefore,  $I_{sp}$  scales with  $C_T$  for fixed  $T_e$ . In addition, although this effect is external to our model, induced electron current should reduce the interaction of the plasma with the thruster walls, thus increasing both  $\eta_m$  and  $I_{sp}$ .

In Fig. 5, we plot the dependencies of plume divergence efficiency and thrust coefficient on the force parameter  $\hat{\Omega}$  at different values of magnetization factor  $\hat{\omega}_{lh}$  and throat radius  $r_e$ . From these figures, we see that both the efficiency and the thrust coefficient grow with  $\hat{\Omega}$  thanks to the focusing of the plasma column. The two parameters show comparable increases, with the thrust coefficient being the parameter



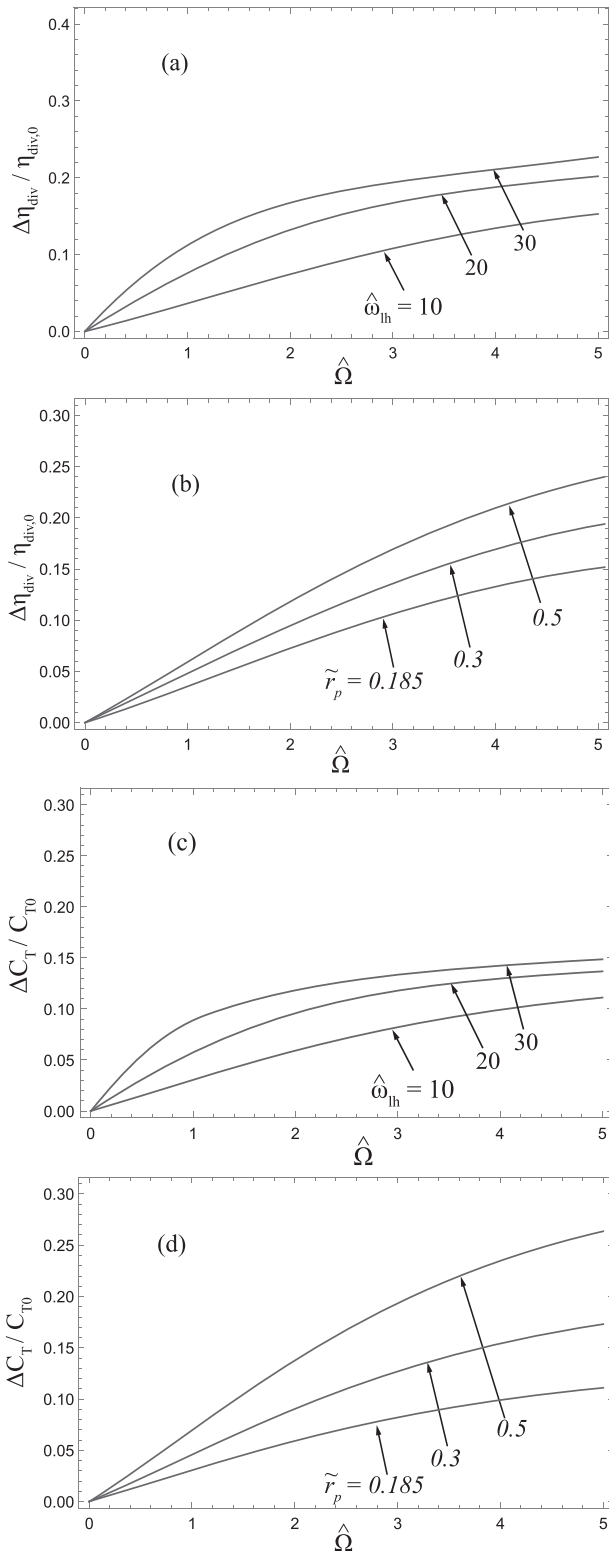


FIG. 5. Relative increase with  $\hat{\Omega}$  of the (a) and (b) nozzle divergence efficiency and the (c) and (d) thrust coefficient. Graphs (a) and (c) are for  $\tilde{r}_p = 0.185$ . Graphs (b) and (d) have  $\hat{\omega}_{lh} = 10$ .  $\tilde{v}_e = 1$  in all cases.

most affected by differences in the normalized plasma radius,  $\tilde{r}_p$ .

An increase in magnetization ( $\hat{\omega}_{lh}$ ) enhances the effect of the swirl, accentuating the knee below  $\hat{\Omega} \approx 2$ . For high values of  $\hat{\Omega}$ , we observe a plateau in the performance enhancement as a function of  $\hat{\omega}_{lh}$ . The performance

enhancement monotonically increases if the curves are parameterized according to  $\tilde{r}_p$ . This might suggest that a high value of  $\hat{\omega}_{lh}$  is advantageous only if  $\hat{\Omega}$  is kept relatively low (i.e., the swirling effect saturates).

In general,  $\eta_{div}$  increases as  $\tilde{r}_p$  decreases.<sup>10,12</sup> Decreasing  $\tilde{r}_p$  requires either a large magnet or a small plasma source. This may not be practical from an engineering standpoint, however, because large magnets imply more weight, and small plasma sources come with increased relative wall losses. From Figs. 5(b) and 5(c), we see that the addition of a focusing stage has a stronger effect for high values of  $\tilde{r}_p$ . In other words, the performance enhancement of the focusing stage is greater for flows that are bounded by highly-divergent flux surfaces. Therefore, the focusing stage may allow for decreased plume divergences without the need for low values of  $\tilde{r}_p$ .

These results imply also that focusing stage is promising not only for propulsion applications but for all magnetic nozzle concepts in which the ability to tune the width of the plasma plume is desirable, e.g., in plasma processing.

## B. Nozzle performance assessment

Because it is an active method for controlling the plasma structure, the focusing stage requires an external source of power to drive the azimuthal electron current. We use the thrust efficiency of the MN as a metric to determine whether the increased divergence efficiency is worth this added power. Thrust efficiency is defined as  $\eta_t \equiv T^2/(2\dot{m}P)$ , where  $T$ ,  $P$ , and  $\dot{m}$  are the thrust, power, and propellant mass flow rate of the thruster.

The ratio of the thrust efficiency of the MN with and without the focusing stage may be written as

$$\frac{\eta_{t,s}}{\eta_{t,0}} = \frac{\eta_{div,s}}{\eta_{div,0}} \left( \frac{1}{1 + P_s/P_0} \right). \quad (28)$$

Here,  $P_s$  and  $P_0$  denote the power required to induce the electron swirl and power of the plasma flow with  $\hat{\Omega} = 0$ , respectively.  $\eta_{div,s}$  and  $\eta_{div,0}$  represent the divergence efficiency with and without electron swirl, respectively.

The MN model used in Sec. III assumed that the electrons remain isothermal throughout the expansion. A known result of this assumption is that an infinite source of heat is required to maintain a constant temperature.<sup>35</sup> In other words,  $P_0 \rightarrow \infty$ , which is clearly non-physical. Assuming instead that the electrons cool according to a polytropic law,  $\mathbf{b} \cdot \nabla(T_e/n^{1/\gamma_e}) = 0$ , the ratio between the focusing stage power and the power in the plasma flow is given by

$$\frac{P_s}{P_0} = \frac{\eta_i}{\eta_s} \left( \frac{\gamma_e - 1}{\gamma_e + 1} \right) \frac{\int_0^1 (\hat{u}_{\theta,e}^2 - \hat{u}_{\theta,e,0}^2) \hat{n}_t(\hat{r}, \hat{\Omega}) \hat{r} d\hat{r}}{\int_0^1 \hat{n}_t(\hat{r}, 0) \hat{r} d\hat{r}}. \quad (29)$$

Here,  $\eta_s$  and  $\eta_i$  are the efficiencies associated with the focusing stage and plasma source, respectively. It is clear that the ratio  $P_s/P_0$  approaches zero for isothermal flow,  $\gamma_e = 1$ , and has a maximum value for adiabatic flow,  $\gamma_e = 5/3$ . In reality, the effective electron polytropic index will fall in between

this range with values near  $\gamma_e \approx 1.2$  observed in experiments.<sup>36,37</sup>

We show in Fig. 6 the thrust efficiency improvement with the focusing stage as a function of the electron swirl,  $\hat{\Omega}$ , for  $\eta_i = \eta_s$ . The curves are obtained for three different values of  $\gamma_e$  by inserting Eq. (29) into Eq. (28). Fig. 6(a) indicates that significant efficiency improvements (in excess of 10%) are possible with a focusing stage for larger values of  $\tilde{r}_p$ . The benefit somewhat diminishes as  $\tilde{r}_p$  decreases, as shown in Fig. 6(b). However, the thrust efficiency with the focusing stage is observed to increase above the nominal value in all cases for the range of  $\hat{\Omega}$  considered here.

We acknowledge the maximum value for the  $\gamma_e = 5/3$  curve in Fig. 6(b). Beyond this maximum, the increased directed kinetic power resulting from the decreased plume divergence is not large enough to compensate for the additional power in the focusing stage. We do not expect this behavior to be a problem in an actual device, however, because the maximum is only observed for adiabatic expansion with relatively low values of  $\tilde{r}_p$  and  $\hat{\omega}_{th}$ , and relatively large  $\hat{\Omega}$ .

It is reasonable to question how the increased thrust power is larger than the power used to drive the azimuthal electron current. Conservation of energy is not violated because the increased thrust power comes from the power that would be otherwise lost to the radial divergence of the plume. This is emphasized by the fact that the performance benefit decreases as the nominal plume divergence decreases, i.e., there is less undirected kinetic power to recover.

We note that the ratio  $P_s/P_0$  is not consistent with  $\eta_{div,s}/\eta_{div,0}$  for  $\gamma_e \neq 1$  because the latter was obtained using an isothermal expansion model. Numerical models suggest that  $\eta_{div}$  increases with  $\gamma_e$ .<sup>35</sup> Therefore, the ratio  $\eta_{div,s}/\eta_{div,0}$  will be somewhat smaller than the values shown in Fig. 6.

Finally, we assess whether or not it is more beneficial for the power used in the focusing stage to be used instead to heat the plasma electrons. If we assume that energy lost to ionization of the incoming propellant is the dominant loss mechanism,<sup>38</sup> the ratio of the thrust efficiency with a

focusing stage to the thrust efficiency with a heating stage can be written as

$$\frac{\eta_{t,s}}{\eta_{t,h}} = \frac{\eta_{th,0}}{\eta_{th,h}} \frac{\eta_{div,s}}{\eta_{div,0}}, \quad (30)$$

where

$$\eta_{th,0} = \frac{1}{1 + 2\epsilon'_i/(\gamma_e g_u^2 T_{e,0})} \quad (31)$$

is the thermal efficiency of the nozzle,  $\epsilon'_i$  is the effective ionization energy, and  $g_u$  is the ratio of the final exhaust velocity to  $c_s$ . We see that  $\eta_{th,h} > \eta_{th,0}$  for  $T_{e,h} > T_{e,0}$ . In other words, the relative contribution of the ionization losses decreases as the electron temperature increases.

Assuming the heating stage adds an amount of power equivalent to  $P_s$  at 100% efficiency, the ratio of the heated electron temperature to the baseline electron temperature is

$$\frac{T_{e,h}}{T_{e,0}} = (1 + P_s/P_0)^{2/3}, \quad (32)$$

which we can combine with Eq. (31) to rewrite Eq. (30) in the following form:

$$\frac{\eta_{t,s}}{\eta_{t,h}} = \frac{\eta_{div,s}}{\eta_{div,0}} \left[ \eta_{th,0} + \frac{1 - \eta_{th,0}}{(1 + P_s/P_0)^{2/3}} \right]. \quad (33)$$

The ratio  $\eta_{t,s}/\eta_{t,h}$  decreases with  $\eta_{th,0}$  because heating has a larger effect at low thermal efficiencies. With that said, we notice that this ratio has a lower bound at  $\eta_{th,0} = 0$ . Specifically,

$$\frac{\eta_{t,s}}{\eta_{t,h}} \geq \frac{\eta_{div,s}}{\eta_{div,0}} \left[ \frac{1}{(1 + P_s/P_0)^{2/3}} \right] \geq \frac{\eta_{t,s}}{\eta_{t,0}}. \quad (34)$$

This inequality suggests that it is more beneficial to drive azimuthal electron current than to heat the electrons as long as the power required to drive the current is less than the gain in directed kinetic exhaust power.

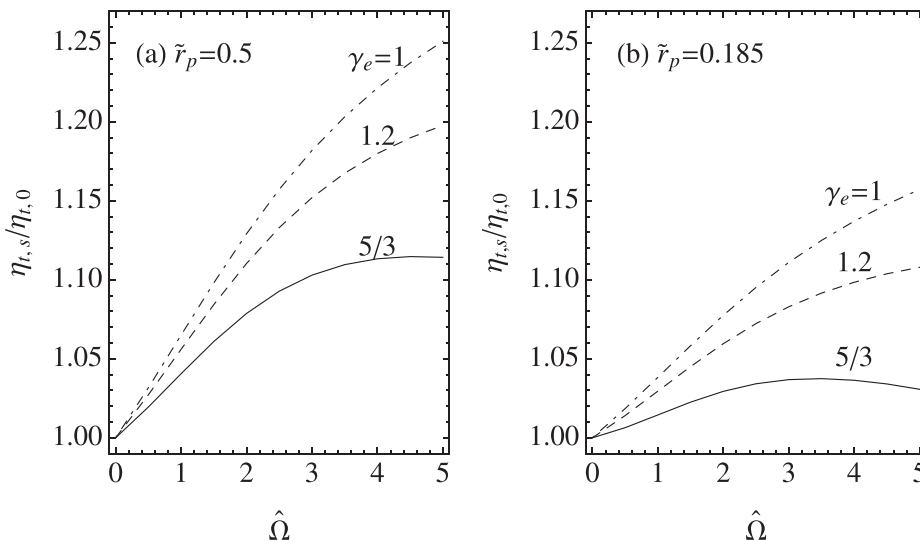


FIG. 6. Ratio between the thrust efficiencies with and without induced diamagnetic electron current as a function of the electron swirl for (a)  $\tilde{r}_p = 0.5$  and (b)  $\tilde{r}_p = 0.185$ . Here,  $\hat{\nu}_e = 1$  and  $\hat{\omega}_{th} = 10$ .

## V. CONCLUSIONS

### A. Relevance to other devices

Magnetic nozzles are intimately related to the cylindrical Hall thruster (CHT).<sup>39</sup> Like the MN that we analyze in this paper, the CHT features a diverging magnetic field with magnetized electrons and un-magnetized ions. One of the two main differences is that a downstream electron-emitting hollow cathode imposes the negative potential drop in the CHT, whereas the negative potential drop in the MN arises from the hot, light electrons outrunning the ions in the axial direction. The other main difference is that the equipotential surfaces of the CHT coincide with the magnetic flux surfaces, whereas for the ideal MN modeled in this paper, the equipotential and magnetic flux surfaces are perpendicular.

Despite these two differences, we can speculate that the mechanism that is the focus of this paper, i.e., MN plume control using induced electron azimuthal motion, can also be applied to the CHT. In fact, Smirnov *et al.*<sup>40</sup> and Raitses<sup>41,42</sup> demonstrated in detail that the plume divergence in a CHT is narrower than would be expected if the ions were accelerated across the magnetic field lines, as would be the case for fully equipotential magnetic surfaces. The decreased plume divergence was shown to result from the natural electron rotation within the device, which conspired to straighten out the electric field.<sup>43</sup> It is thus reasonable to suspect that actively augmenting the natural electron rotation could further reduce the plume divergence for the CHT.

Electron rotation in a MN may be induced using a radial electric field upstream from the diverging magnetic field. A simple way to do this, which we will present in an upcoming paper, is to apply a DC voltage between central and annular electrodes. We suspect that this method could be reasonably expected to work in a CHT as well. Note that this suggestion differs from the use of additional electrodes in previous Hall thruster studies,<sup>44</sup> which have placed electrodes at the plasma periphery to control the axial, rather than radial electric field.

### B. Concluding remarks

We assessed the effects of an azimuthal current induced at the throat of an electron-driven magnetic nozzle on the plasma flow through the nozzle using a finite-temperature two-dimensional axisymmetric model where the modified equilibrium conditions at the throat were evaluated through the introduction of an azimuthal body force on the electrons and an analytical approximation was used to obtain the solution. We found that the effect of the azimuthal current on the plume leads to a modification of the radial density profile and thus can only be represented by a finite-temperature model.

We evaluated the resulting propulsive performance of the magnetic nozzle in terms of nozzle divergence efficiency, thrust coefficient, and nozzle thrust efficiency and found that all these parameters are enhanced by the confining effect of the applied azimuthal force. Stronger enhancements were observed for higher plume magnetization. We also found that the introduction of an azimuthal force is more

effective at raising the efficiency than a direct increase of the total jet power through heating.

These findings illustrate the promise of using an azimuthal-current-driven beam focusing stage for enhancing the propulsive performance of magnetic nozzles. Furthermore, this focusing stage may be extended to similar electric propulsion devices, namely, the cylindrical Hall thruster.

## ACKNOWLEDGMENTS

The authors would like to thank Professor Nat Fisch for insightful comments regarding relevance to other devices. The work of the first author has been supported by the scholarship *Borsa di Studio Tesi All'Estero 2012-2013* of the Politecnico di Milano. We also thank the Program in Plasma Science and Technology for support through DOE Contract No. DE-AC02-09CH11466 and the Department of Defense (DoD) National Defense Science and Engineering Graduate Fellowship (NDSEG) Program.

- <sup>1</sup>S. A. Cohen, X. Sun, N. M. Ferraro, E. E. Scime, M. Miah, S. Stange, N. S. Siefert, and R. F. Boivin, *IEEE Trans. Plasma Sci.* **34**, 792 (2006).
- <sup>2</sup>R. Hoyt, J. Scheuer, K. Schoenberg, R. Gerwin, R. Moses, and I. Henins, *IEEE Trans. Plasma Sci.* **23**, 481 (1995).
- <sup>3</sup>K. F. Schoenberg, R. A. Gerwin, R. W. Moses, Jr., J. T. Scheuer, and H. P. Wagner, *Phys. Plasmas* **5**, 2090 (1998).
- <sup>4</sup>J. Reece Roth, *Industrial Plasma Engineering: Volume 2—Applications to Nonthermal Plasma Processing* (CRC Press, Boca Raton, FL, 2001).
- <sup>5</sup>C. S. Olsen, M. G. Ballenger, M. D. Carter, F. R. Chang Díaz, M. Giambusso, T. W. Glover, A. V. Ilin, J. P. Squire, B. W. Longmire, E. A. I. Bering, and P. A. Cloutier, in Proceedings of the 33rd International Electric Propulsion Conference, Washington, D.C. 6–10 Oct. 2013.
- <sup>6</sup>E. B. Hooper, *J. Propul. Power* **9**, 757 (1993).
- <sup>7</sup>R. W. Moses, R. A. Gerwin, and K. F. Schoenberg, in Proceedings of the 9th Symposium on Space Nuclear Power Systems, Albuquerque, New Mexico, 12–16 January 1992.
- <sup>8</sup>J. M. Little and E. Y. Choueiri, in Proceedings of the 47th AIAA/ASME/SAE/ASEE Joint Propulsion Conference, San Diego, CA, 31-July–3-Aug. 2011.
- <sup>9</sup>P. F. Schmit and N. J. Fisch, *J. Plasma Phys.* **75**, 359 (2009).
- <sup>10</sup>E. Ahedo and M. Merino, *Phys. Plasmas* **17**, 073501 (2010).
- <sup>11</sup>E. Ahedo and M. Merino, *Phys. Plasmas* **19**, 083501 (2012).
- <sup>12</sup>J. M. Little and E. Y. Choueiri, *Phys. Plasmas* **20**, 103501 (2013).
- <sup>13</sup>H. Alfvén, *Space Phys.* **81**, 4019 (1976).
- <sup>14</sup>C. Charles, K. Takahashi, and R. W. Boswell, *Appl. Phys. Lett.* **100**, 113504 (2012).
- <sup>15</sup>B. W. Longmire and J. P. Sheehan, in Proceedings of the 40th IEEE International Conference on Plasma Science, San Francisco, CA, USA, 16–21 June 2013.
- <sup>16</sup>N. Sakaguchi, Y. Kajimura, and H. Nakashima, *Trans. Jpn. Soc. Aeronaut. Space Sci.* **48**, 180 (2005).
- <sup>17</sup>J. F. Santarius and B. G. Logan, *J. Propul. Power* **14**, 519 (1998).
- <sup>18</sup>W. Von Jaskowsky, A. J. Kelley, R. G. Jahn, and J. E. Polk, *J. Propul. Power* **3**, 33 (1987).
- <sup>19</sup>K. Kuriki and O. Okada, *Phys. Fluids* **13**, 2262 (1970).
- <sup>20</sup>E. Ahedo and M. Merino, in Proceedings of the 48th AIAA/ASME/SAE/ASEE Joint Propulsion Conference, Atlanta, Georgia, 29 July–1 August 2012.
- <sup>21</sup>A. V. Arefiev and B. N. Breizman, *Phys. Plasmas* **12**, 043504 (2005).
- <sup>22</sup>C. A. Deline, R. D. Bengtson, B. B. Breizman, M. R. Tushentsov, J. E. Jones, D. G. Chavers, C. C. Dobson, and B. M. Schuettpelz, *Phys. Plasmas* **16**, 033502 (2009).
- <sup>23</sup>E. Ahedo, *Plasma Phys. Controlled Fusion* **53**, 124037 (2011).
- <sup>24</sup>R. A. Clemente, *J. Phys. Soc. Jpn.* **67**, 3450 (1998).
- <sup>25</sup>W. N. Hugrass, *Plasma Phys. Controlled Fusion* **42**, 1219 (2000).
- <sup>26</sup>W. N. Hugrass, *Plasma Phys. Controlled Fusion* **45**, 209 (2003).
- <sup>27</sup>E. Ahedo, *Phys. Plasmas* **16**, 113503 (2009).
- <sup>28</sup>E. Ahedo, *Phys. Plasmas* **18**, 103506 (2011).
- <sup>29</sup>L. C. Steinhauer, *Phys. Plasmas* **8**, 3367 (2001).

- <sup>30</sup>A. Fruchtman, G. Makrinich, and J. Ashkenazy, [Plasma Sources Sci. Technol.](#) **14**, 152 (2005).
- <sup>31</sup>R. A. Gerwin, "Integrity of the plasma magnetic nozzle," Technical Report No. TP-2009-213439 (NASA, 2009).
- <sup>32</sup>P. Chabert and N. Braithwaite, *Physics of Radio-Frequency Plasmas* (Cambridge University Press, Cambridge, 2011) p. 274.
- <sup>33</sup>B. N. Breizman and A. V. Arefiev, [Phys. Rev. Lett.](#) **84**, 3863 (2000).
- <sup>34</sup>J. M. Little and E. Y. Choueiri, *IEEE Trans. Plasma Sci.* **PP**(99), 1.1 (2014).
- <sup>35</sup>M. Merino and E. Ahedo, *IEEE Trans. Plasma Sci.* **PP**(99), 1.1 (2014).
- <sup>36</sup>K. Yoshida, T. Kanuma, H. Ichii, A. Nezu, H. Matsuura, and H. Akatsuka, [IEEE Trans. Electr. Electr. Eng.](#) **4**, 416 (2009).
- <sup>37</sup>J. M. Little and E. Y. Choueiri, in Proceedings of the 50th AIAA/ASME/SAE/ASEE Joint Propulsion Conference, Cleveland, Ohio, 28–30 July 2014.
- <sup>38</sup>E. Ahedo and J. Navarro-Cavallé, [Phys. Plasmas](#) **20**, 043512 (2013).
- <sup>39</sup>Y. Raitses and N. J. Fisch, [Phys. Plasmas](#) **8**, 2579 (2001).
- <sup>40</sup>A. Smirnov, Y. Raitses, and N. J. Fisch, [Phys. Plasmas](#) **14**, 057106 (2007).
- <sup>41</sup>Y. Raitses, A. Smirnov, and N. J. Fisch, [Appl. Phys. Lett.](#) **90**, 221502 (2007).
- <sup>42</sup>Y. Raitses, A. Smirnov, and N. J. Fisch, [Phys. Plasmas](#) **16**, 057106 (2009).
- <sup>43</sup>N. J. Fisch, A. Fruchtman, and Y. Raitses, [Plasma Phys. Controlled Fusion](#) **53**, 124038 (2011).
- <sup>44</sup>A. Fruchtman, N. J. Fisch, and Y. Raitses, [Phys. Plasmas](#) **8**, 1048 (2001).